

On factorization, quark counting and vector dominance

M. M. Block

Department of Physics and Astronomy,
Northwestern University, Evanston, IL 60208

F. Halzen^y

Department of Physics,
University of Wisconsin, Madison, WI 53706

G. Pancheri

INFN-Laboratori Nazionali di Frascati,
Frascati, Italy

Abstract

Using an eikonal structure for the scattering amplitude, Block and Kaidalov [1] have derived factorization theorems for nucleon-nucleon, p and \bar{p} scattering at high energies, using only some very general assumptions. We present here an analysis giving experimental confirmation for factorization of cross sections, nuclear slope parameters B and α -values (ratio of real to imaginary portion of forward scattering amplitudes), showing that:

- the three factorization theorems [1] hold,
- the additive quark model holds to 1% ,
- and vector dominance holds to better than 4% .

^yWork partially supported by Department of Energy contract DA-AC02-76-ER02289 Task D.

^yWork partially supported by Department of Energy Grant No. DE-FG02-95ER40896 and the University of Wisconsin Research Committee with funds granted by the Wisconsin Alumni Research Foundation.

1 Introduction

Assuming factorizable eikonals in impact parameter space b for nucleon-nucleon, p and \bar{p} scattering processes whose opacities are equal, Block and Kaidalov [1] have proved three factorization theorems:

$$1. \quad \frac{\sigma_{nn}(s)}{\sigma_p(s)} = \frac{\sigma_{\bar{p}}(s)}{\sigma(s)};$$

where the σ 's are the total cross sections for nucleon-nucleon, p and \bar{p} scattering,

$$2. \quad \frac{B_{nn}(s)}{B_p(s)} = \frac{B_{\bar{p}}(s)}{B(s)};$$

where the B 's are the nuclear slope parameters for elastic scattering,

$$3. \quad \frac{\rho_{nn}(s)}{\rho_p(s)} = \frac{\rho_{\bar{p}}(s)}{\rho(s)};$$

where the ρ 's are the ratio of the real to imaginary portions of the forward scattering amplitudes,

with each factorization theorem having its own proportionality constant. These theorems are exact, for all s (where \sqrt{s} is the c.m.s. energy), and survive exponentiation of the eikonal [1].

Physically, the assumption of equal opacities, where the opacity is defined as the value of the eikonal at $b=0$, is the same as demanding that the ratios of elastic to total cross sections are equal, i.e.,

$$\frac{\sigma_{el}}{\sigma_{tot}} = \frac{\sigma_{el}}{\sigma_{tot}} = \frac{\sigma_{el}}{\sigma_{tot}}; \quad (1)$$

as the energy goes to infinity [1].

Factorization theorem 1, involving ratios of cross sections, is perhaps the best known. Factorization theorems 2 and 3 are less known, but turn out to be of primary importance. The purpose of this note is to present strong experimental evidence for all three factorization theorems, as well as evidence for the additive quark model and vector dominance.

2 Eikonal Model

In an eikonal model [5], a (complex) eikonal $\chi(b;s)$ is defined such that $a(b;s)$, the (complex) scattering amplitude in impact parameter space b , is given by

$$a(b;s) = \frac{i}{2} \int_{-R}^R \chi(b;s) d^2b = \frac{i}{2} \int_{-R}^R [1 - e^{-i\chi(b;s)}] d^2b; \quad (2)$$

Using the optical theorem, the total cross section $\sigma_{tot}(s)$ is given by

$$\sigma_{tot}(s) = 2 \int_{-R}^R [1 - \cos(\chi(b;s))] d^2b; \quad (3)$$

the elastic scattering cross section $\sigma_{el}(s)$ is given by

$$\sigma_{elastic}(s) = \int_{-R}^R [1 - e^{-i\chi(b;s)}] d^2b; \quad (4)$$

and the inelastic cross section, $\sigma_{inelastic}(s)$, is given by

$$\sigma_{inelastic}(s) = \sigma_{tot}(s) - \sigma_{elastic}(s) = \int_{-R}^R [1 - e^{-2\chi(b;s)}] d^2b; \quad (5)$$

The ratio of the real to the imaginary part of the forward nuclear scattering amplitude, ρ , is given by

$$\rho(s) = \frac{\text{Re } i \int_{-R}^R [1 - e^{-i\chi(b;s)}] d^2b}{\text{Im } i \int_{-R}^R [1 - e^{-i\chi(b;s)}] d^2b} \quad (6)$$

and the nuclear slope parameter B is given by

$$B = \frac{\int_{-R}^R b^2 a(b;s) d^2b}{2 \int_{-R}^R a(b;s) d^2b}; \quad (7)$$

2.1 Even Eikonal

A description of the forward proton-proton and proton-antiproton scattering amplitudes is required which is analytic, unitary, satisfies crossing symmetry and the Froissart bound. A convenient parameterization [2, 5] consistent with the above constraints and with the high-energy data can be constructed in a model where the asymptotic nucleon becomes a black disk as a reaction of particle (jet) production. The increase of the total cross section is the shadow of jet-production which is parameterized in parton language. The picture does not reproduce the lower energy data which is simply parameterized using Regge phenomenology. The even QCD-inspired eikonal even for nucleon-nucleon scattering [2, 5] is given by the sum of three contributions, gluon-gluon, quark-gluon and quark-quark, which are individually factorizable into a product of a cross section $\sigma(s)$ times an impact parameter space distribution function $W(b; s)$, i.e.,:

$$\begin{aligned} e^{i\chi_{\text{even}}(s;b)} &= e^{i\chi_{gg}(s;b)} + e^{i\chi_{qg}(s;b)} + e^{i\chi_{qq}(s;b)} \\ &= i \chi_{gg}(s) W(b; \chi_{gg}) + \chi_{qg}(s) W(b; \sqrt{\chi_{qg}}) + \chi_{qq}(s) W(b; \sqrt{\chi_{qq}}); \end{aligned} \quad (8)$$

where the impact parameter space distribution function is the convolution of a pair of dipole form factors:

$$W(b; s) = \frac{1}{96} (b^2)^3 K_3(b^2); \quad (9)$$

It is normalized so that $\int_0^R W(b; s) d^2b = 1$: Hence, the χ 's in eq. (8) have the dimensions of a cross section. The factor i is inserted in eq. (8) since the high energy eikonal is largely imaginary (the value for nucleon-nucleon scattering is rather small).

The opacity of the eikonal, its value at $b=0$, is given by

$$\sigma^{\text{nn}} = \frac{i}{12} [\chi_{gg}(s) + \chi_{qg}(s) + \chi_{qq}(s)]; \quad (10)$$

a simple sum of the products of the appropriate cross sections with the χ 's, a result which we will utilize later.

The totaleven contribution is not yet analytic. For large s , the even amplitude in eq. (8) is made analytic by the substitution (see the table on p. 580 of reference [3], along with reference [4]) $s \rightarrow \sqrt{s}$: The quark contribution $\chi_{qq}(s;b)$ accounts for the constant cross section and a Regge descending component ($\propto 1/\sqrt{s}$), whereas the mixed quark-gluon term $\chi_{qg}(s;b)$ simulates diffraction ($\propto \log s$). The gluon-gluon term $\chi_{gg}(s;b)$, which eventually rises as a power law s , accounts for the rising cross section and dominates at the highest energies. In eq. (8), the inverse sizes (in impact parameter space) χ_{qq} and χ_{qg} are to be fixed by experiment, whereas the quark-gluon inverse size is taken as $\sqrt{\chi_{qg}}$. For more detail, see ref. [5].

2.2 Odd Eikonal

The high energy analytic odd amplitude (for its structure in s , see eq. (5.5b) of reference [3], with $\alpha = 0.5$) that fits the data is given by [5]

$$\chi_{\text{odd}}(b; s) = \chi_{\text{odd}} W(b; \chi_{\text{odd}}); \quad (11)$$

with $\chi_{\text{odd}} \propto 1/\sqrt{s}$, and with

$$W(b; \chi_{\text{odd}}) = \frac{1}{96} (\chi_{\text{odd}} b^2)^3 K_3(\chi_{\text{odd}} b^2); \quad (12)$$

normalized so that $\int_0^R W(b; \chi_{\text{odd}}) d^2b = 1$:

2.3 Total Eikonal

The data for both pp and pp are fitted using the totaleikonal

$$\chi_{\text{pp}}^{\text{pp}} = \chi_{\text{even}} + \chi_{\text{odd}}; \quad (13)$$

3 A G lobal F it of A ccelerator and C osm ic R ay D ata

U sing an eikonal analysis in in pact param eter space, B lock et al. [2, 5, 9] have constructed a Q CD -inspired param eterization of the forward proton {proton and proton {antiproton scattering amplitudes which ts all accelerator data [6] for σ_{tot} , nuclear slope param eter B and ρ , the ratio of the real-to-im aginary part of the forward scattering am plitude for both pp and pp collisions, using a χ^2 procedure and the eikonal of eq. (13); see F ig.1 and F ig.2 which are taken from ref. [9]] in addition, the high energy cosm ic ray cross sections

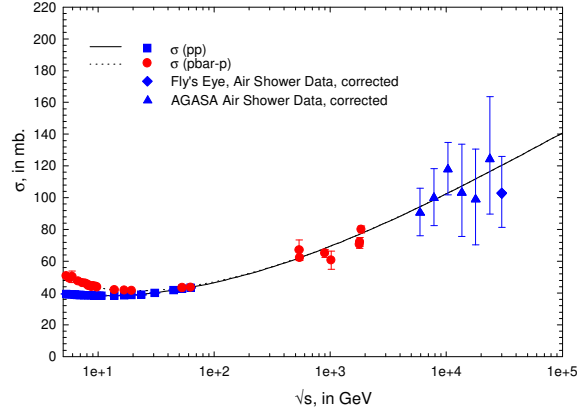


Figure 1: The tted σ_{pp} and $\sigma_{p\bar{p}}$, in mb vs. \sqrt{s} , in GeV, for the Q CD -inspired t of total cross section, B and ρ for both pp and pp. The accelerator data (squares are pp and circles are p \bar{p}) and the cosm ic ray points (diamond, Fly's Eye and triangles, AGASA) have been tted simultaneously. The cosm ic ray data that are shown have been converted from $\sigma_{p\text{air}}^{inel}$ to σ_{pp} .

of Fly's Eye [7] and AGASA [8] experim ents are also simultaneously t[9]. Because the param eterization is both unitary and analytic, its high energy predictions are e ctively m odel-independent, if you require that the proton is asymptotically a black disk. A m ajor difference between simultaneously tting the cosm ic ray and accelerator data and earlier results in which only accelerator data were used, is a lowering (by about a factor of 2.5) of the error of the predictions for the high energy cross sections. In particular, the error in σ_{pp} at $\sqrt{s} = 30$ TeV is reduced to 1.5 %, because of signi cant reductions in the errors estimated for the t param eters (for a m ore com plete explanation, see ref. [9]).

The plot of σ_{pp} vs. \sqrt{s} , including the cosm ic ray data, is shown in F ig.1, which was taken from ref. [9]. The overall agreement between the accelerator and the cosm ic ray pp cross sections w ith the Q CD -inspired t, as shown in F ig.1, is striking.

In brief, the eikonal description provides an excellent description of the experim ental data at high energy for both pp and pp scattering at high energies.

4 Factorization

W e em phasize that the Q CD -inspired param eterization of the pp and pp data [2, 5, 9] allow s us to calculate accurately the even eikonal of eq. (8) needed for:

the total cross section σ_{nn} (from eq. (3)) used in the factorization theorem 1,

the nuclear slope param eter B_{nn} (from eq. (7)) used in the factorization theorem 2,

and the ρ -value ρ_{nn} (from eq. (6)) used in the factorization theorem 3,

since we m ust com pare σ_{nn} to σ_{pp} and $\sigma_{p\bar{p}}$ reactions.

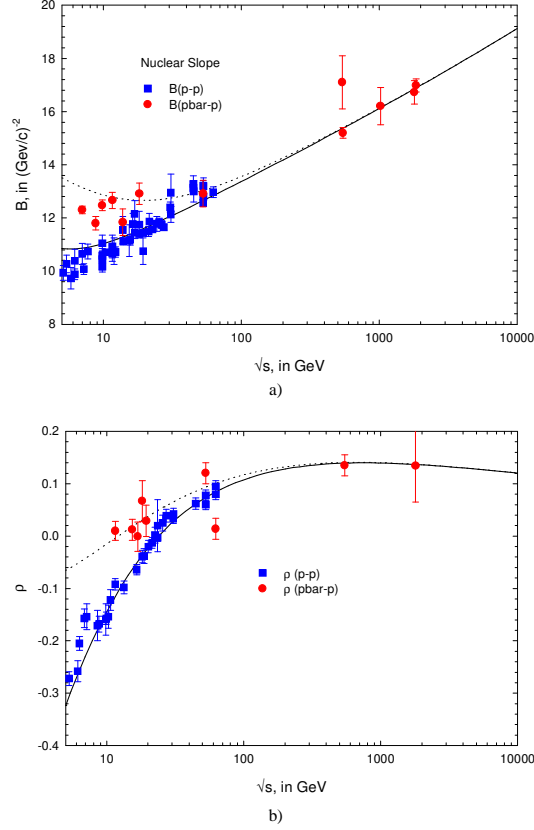


Figure 2: The fitted values for the nuclear slope parameters B_{pp} and $B_{p\bar{p}}$, in $(\text{GeV}/c)^2$ vs. \sqrt{s} , in GeV, for the QCD-inspired fit are shown in (a). In (b), the fitted values for ρ_{pp} and $\rho_{p\bar{p}}$ are shown.

4.1 Theorems

As shown in ref. [1], the eikonals for p and \bar{p} scattering that satisfy eq. (1) are given by

$$N(s; b) = i \left[\frac{1}{2} W_{gg}(s; \frac{1}{2}) + \frac{1}{2} W_{qg}(s; \frac{1}{2}) + \frac{1}{2} W_{qq}(s; \frac{1}{2}) \right]; \quad (14)$$

and

$$N(s; b) = i \left[\frac{1}{2} W_{gg}(s; \frac{1}{2}) + \frac{1}{2} W_{qg}(s; \frac{1}{2}) + \frac{1}{2} W_{qq}(s; \frac{1}{2}) \right]; \quad (15)$$

where we obtain N from N^{even} from multiplying each in N^{even} by $\frac{1}{2}$ and each N^{odd} by $\frac{1}{2}$, and, in turn, we next obtain N from N^{even} from multiplying each in N^{even} by $\frac{1}{2}$ and each N^{odd} by $\frac{1}{2}$. The N in eq. (14) and eq. (15) is an energy-independent proportionality constant. The functional forms of the impact parameter distributions are assumed to be the same for p , \bar{p} and nn reactions. It is clear from using eq. (9), eq. (14), eq. (15) and then comparing to the opacity of eq. (10), that the three opacities are all the same, i.e.,

$$O^{nn} = O^p = O^{\bar{p}} = \frac{1}{12} \left[W_{gg}(s) \frac{1}{2} + W_{qg}(s) \frac{1}{2} + W_{qq}(s) \frac{1}{2} \right]; \quad (16)$$

Hence, from ref. [1], we have the three factorization theorems

$$\frac{N^{nn}(s)}{N^p(s)} = \frac{N^{\bar{p}}(s)}{N^p(s)} \quad (17)$$

$$\frac{B_{nn}(s)}{B_p(s)} = \frac{B_p(s)}{B_p(s)} \quad (18)$$

$$\frac{B_{nn}(s)}{B_p(s)} = \frac{B_p(s)}{B_p(s)}; \quad (19)$$

valid for all s . It is easily inferred from ref. [1] that

$$B_{nn}(s) = P_{had} B_p(s) = (P_{had})^2 B_{nn}(s) \quad (20)$$

$$B_p(s) = B_p(s) = B_{nn}(s) \quad (21)$$

$$B_p(s) = B_p(s) = B_{nn}(s); \quad (22)$$

where P_{had} is the probability that a photon transforms into a hadron, assumed to be independent of energy and B is a proportionality constant, also independent of energy. The value of B , of course, is model-dependent. For the case of the additive quark model, $B = \frac{2}{3}$.

We emphasize the importance of the result of eq. (22) that the B 's are all equal, independent of the assumed value of B , i.e., the equality does not depend on the assumed model.

4.2 Experimental Verification of Factorization using Compton Scattering

The solid curve in Fig. 3 is B_{nn} , plotted as a function of the c.m. energy \sqrt{s} . According to eq. (22), this

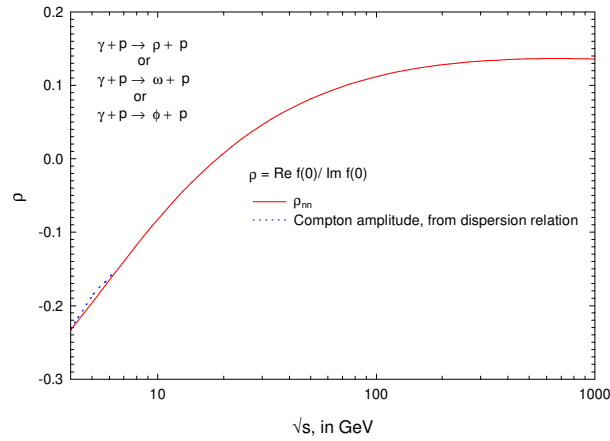


Figure 3: The solid curve is B_{nn} , the predicted ratio of the real to imaginary part of the forward scattering amplitude for the 'elastic' reactions, $\gamma + p \rightarrow V + p$ scattering amplitude, where V is ρ , ω or ϕ (using the factorization theorem of eq. (22)). The dotted curve is ratio of the real to imaginary part of the forward scattering amplitude for Compton scattering, $\gamma + p \rightarrow \gamma + p$, found from dispersion relations [10]. It has been slightly displaced from the solid curve for clarity in viewing.

should be the same as B_p . No experimental data for the 'elastic scattering' reactions $\gamma + p \rightarrow V + p$, where V is the vector meson ρ , ω or ϕ , are available for direct comparison. However, Damashek and Gilman [10] have calculated the value for Compton scattering $\gamma + p \rightarrow \gamma + p$ using dispersion relations, i.e., the true elastic scattering reaction for photon-proton scattering. The dispersion relation calculation gives B_p if we assume that it is the same as that for the 'elastic scattering' reactions $\gamma + p \rightarrow V + p$. In this picture we expect that $B_p = B_{nn} = B_{nn} = B_{nn}$. We then compare the dispersion relation calculation, the dotted line in Fig. 3, with our prediction for B_p from eq. (22) (B_{nn} , the solid line taken from ref. [9]). The agreement is so close that the two curves had to be moved apart so that they may be viewed more clearly. It is clearly of importance to extend the energy region of the dispersion calculation. However, over the limited energy range available from the dispersion calculation, the prediction from eq. (22) of equal B -values is well verified experimentally.

4.3 Quark Counting

The additive quark model tells us from quark counting that in eq. (21) is given by $\alpha = \frac{2}{3}$. We can experimentally determine α by invoking from eq. (21) the relation $B_p = B_{nn}$ (B_{nn} is computed using the parameters from ref. [9]), and fitting α . In our picture, the ‘elastic scattering’ reactions $\gamma + p \rightarrow V + p$, where V is the vector meson ρ , ω or ϕ , require that $B = B_\rho = B_\omega (= B_\phi)$. To determine the value of α in the relation $B_p = B_{nn}$, a χ^2 fit was made to the available B_p data. In Fig. 4 we plot B_{nn} vs. the c.m.s. energy \sqrt{s} , using the best-fit value of $\alpha = 0.661 \pm 0.008$, against the experimental values of B_p . The fit gave $\chi^2 = 16.4$ for 10 degrees of freedom. Inspection of Fig. 4 shows that the experimental point of B at $\sqrt{s} = 5.2$ GeV which contributes 6.44 to the χ^2 clearly cannot lie on any smooth curve and thus can safely be ignored. Neglecting the contribution of this point gives a $\chi^2/\text{d.f.} = 0.999$, a very satisfactory result. We emphasize that the experimental B_p data thus

require $\alpha = 0.661 \pm 0.008$, a 1% measurement in excellent agreement with the value of $2/3$ that is obtained from the additive quark model.

clearly verify the nuclear slope factorization theorem of eq. (21) over the available energy range spanned by the data.

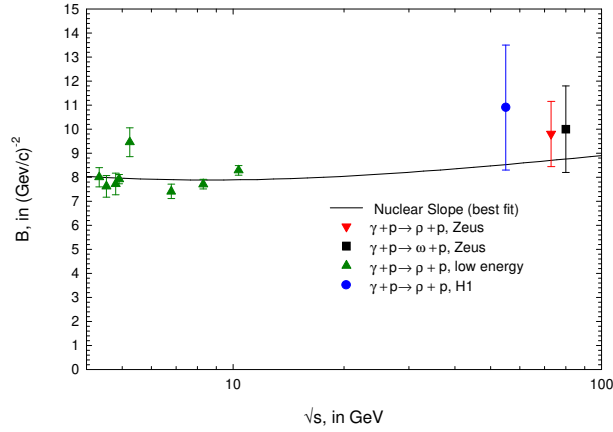


Figure 4: A χ^2 fit of experimental data for the nuclear slopes B , from the ‘elastic scattering’ reactions $\gamma + p \rightarrow V + p$, where V is ρ , ω or ϕ , to the relation $B_p = B_{nn}$, of eq. (21), where $\alpha = 0.661 \pm 0.008$

For additional evidence involving the equality of the nuclear slopes B_ρ , B_ω and B_ϕ from differential elastic scattering data $\frac{d}{dt}$, see Figures (13,14,15) of ref. [5].

4.4 Vector Dominance, using γp Cross Sections

Using $\alpha = \frac{2}{3}$ and eq. (20), we write

$$P_p(s) = \frac{2}{3} P_{had-nn}(s); \quad (23)$$

where P_{had} is the probability that a photon will interact as a hadron. We will use the value $P_{had} = 1/240$. This value is approximately 4% greater than that derived from vector dominance, $1/249$. Using (see Table XXXV, pag. 393 of ref. [11]) $f^2_{\rho^0} = 2.2$, $f^2_{\omega} = 23.6$ and $f^2_{\phi} = 18.4$, we find $\sum_V (4 = f_V^2) = 1/249$, where $V = \rho^0, \omega, \phi$. The value we use of $1/240$ is found by normalizing the total γp cross section to the low energy data and is illustrated in Fig. 5, where we plot the total cross section for $\gamma + p \rightarrow$ hadrons from eq. (23) as a function of the c.m.s. energy \sqrt{s} . The values for B_{nn} have been deduced from the results of ref. [9], using the even eikonal from eq. (8). The fit is exceptionally good, reproducing the rising cross section for γp , using the parameters fixed by nucleon-nucleon scattering. The fact that we use the value $1/240$ rather

than $1/249$ (4% greater than the vector meson prediction) reflects the fact that P_{had} , the total probability that the photon is a hadron, should have a small contribution from the continuum, as well as from the vector mesons ρ , ω and ϕ . Thus, within the uncertainties of our calculation, the experimental data in the ρ sector

are compatible with vector meson dominance.

agree with cross section factorization theorem of eq. (20).

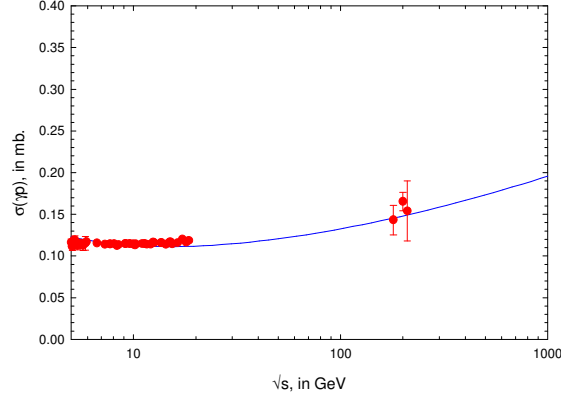


Figure 5: The total cross section for ρ scattering. The solid curve is the predicted total cross section from the factorization relation of eq. (20), $\sigma_{\rho} = \frac{2}{3}P_{\text{had}}\sigma_{\text{nn}}$, where $P_{\text{had}} = 1/240$.

4.5 Experimental Verification of Factorization using $\gamma\gamma$ Scattering

Using quark counting and the factorization theorem of eq. (20), we now write $\sigma_{\gamma\gamma} = \frac{2}{3}P_{\text{had}}\sigma_{\text{nn}}$ where $P_{\text{had}} = 1/240$. In Fig. 6 we plot our factorization prediction for $\sigma_{\gamma\gamma}$ (s) as a function of the c.m.s. energy

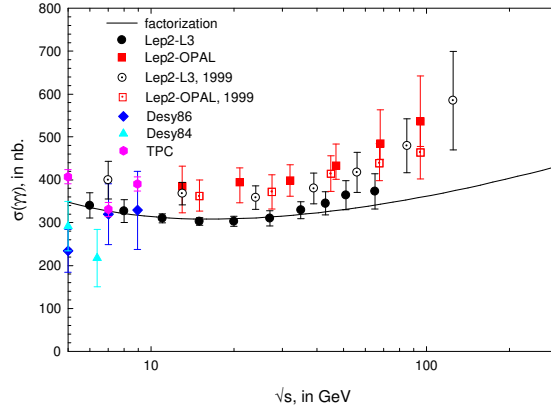


Figure 6: The predicted total cross section for $\gamma\gamma$ scattering from the factorization theorem of eq. (20), $\sigma_{\gamma\gamma} = \frac{2}{3}P_{\text{had}}\sigma_{\text{nn}}$, where $P_{\text{had}} = 1/240$. The data sources are indicated in the legend.

P_{had} and compare it to various sets of experimental data. It is clear that factorization, as expressed in eq. (20), selects the preliminary L3 data (solid circles) rather than the preliminary OPAL results (solid squares) [12]. The Monte Carlo-averaged final results of L3, given by the open circles, agrees, within errors,

with the revised OPAL data, with both new sets having a normalization of about 15-20 % higher than the factorization prediction given by the solid line. The major difference between the earlier L3 result and the revised data was the use of the average normalization from the output of two different Monte Carls. We find it remarkable that the cross section factorization theorem of eq. (20), using only input from the additive quark model and vector meson dominance, gives a reasonable prediction of the experimental data over a cross section magnitude span of more than a factor of 10^5 and an energy region of $3 \sqrt{s} = 100 \text{ GeV}$.

5 Conclusions

The available data on nn , p and \bar{p} reactions lend strong experimental support to the factorization hypotheses of

- the well-known cross section factorization theorem of eq. (17) and eq. (20),
- the lessor-known nuclear slope factorization theorem of eq. (18) and eq. (21),
- the relatively obscure requirement of eq. (22) that $\sigma_{nn} = \sigma_{p\bar{p}} = \sigma_{\bar{p}p}$,

as well as

verifying the additive quark model by measuring $\sigma_{\bar{p}p} = 0.661 \pm 0.008$, a result within 1% of the value of $2/3$ expected for the quark model, using B_p measurements over a wide span of energies, $3 \sqrt{s} = 200$.

confirming vector dominance using σ_{nn} , p and \bar{p} over an energy region of $3 \sqrt{s} = 100 \text{ GeV}$ and a cross section factor of over 10^5 .

References

- [1] M. M. Block and A. B. Kaidalov, "Consequences of the Factorization Hypothesis in pp ; pp ; p and Collisions", ePrint Archive: hep-ph/0012365, Phys. Rev. D 64, 076002 (2001).
- [2] M. M. Block et al, Phys. Rev. D 45, 839 (1992).
- [3] M. M. Block and R. N. Cahn, Rev. Mod. Phys. 57, 563 (1985).
- [4] Eden, R. J., "High Energy Collisions of Elementary Particles", Cambridge University Press, Cambridge (1967).
- [5] M. M. Block et al, ePrint Archive: hep-ph/9809403, Phys. Rev. D 60, 054024 (1999).
- [6] The accelerator data of the new E-811 high energy cross section at the Tevatron has been included: C. Avila et al, Phys. Lett. B 445, 419 (1999).
- [7] R. M. Baltrusaitis et al, Phys. Rev. Lett. 52, 1380 (1984).
- [8] M. Honda et al, Phys. Rev. Lett. 70, 525 (1993).
- [9] M. M. Block et al, ePrint Archive: hep-ph/0004232, Phys. Rev. D 62, 077501 (2000).
- [10] M. Damaskus and F. J. Gilman, Phys. Rev. D 1, 1319 (1970).
- [11] T. H. Bauer et al, Rev. Mod. Phys. 50, 261 (1978).
- [12] PLUTO Collaboration, Ch. Berger et al, Phys. Lett. B 149, 421 (1984); TPC/2 Collaboration, H. Aihara et al, Phys. Rev. D 41, 2667 (1990); MD-1 Collaboration, S. E. Barz et al, Z. Phys. C 53, 219 (1992); L3 Collaboration, M. Acciarri et al, Phys. Lett. B 408, 450 (1997); F. Wackerle, "Total Hadronic Cross-Section for Photon-Photon Interactions at LEP", to be published in the Proceedings of the XXV II International Symposium on Multiparticle Dynamics, Frascati, September 1997, and Nucl. Phys. B, Proc. Suppl.